CHEMICAL ENGINEERING TRANSACTIONS
VOL. 114, 2024
A publication of AIDIC
The Italian Association of Chemical Engineering
Online at www.cetjournal.it
Guest Editors: Petar S. Varbanov, Min Zeng, Yee Van Fan, Xuechao Wang
Copyright © 2024, AIDIC Servizi S.r.l.
ISBN 979-12-81206-12-0; **ISSN** 2283-9216
DOI: 10.3303/CET24114184

Polypyrrole as a Nanofiller: Comparative Effects on the Properties of Polycaprolactone Scaffolds for Potential Myocardial Tissue Applications

Ana M. Muñoz-González[a,*], Dianney Clavijo-Grimaldo[b]

[a]Faculty of Engineering, Universidad Nacional de Colombia; Bogotá, Colombia. ORCID: 0000-0002-3191-9891
[b]School of Medicine, Universidad Nacional de Colombia; Bogotá, Colombia.
anmmunozgo@unal.edu.co

This study investigates the incorporation of polypyrrole (PPy) as a nanofiller in polycaprolactone (PCL) electrospun nanofiber scaffolds for potential application in cardiac tissue engineering (CTE). Characterization techniques including SEM, FTIR, tensile strength testing, and contact angle measurements were employed. PPy incorporation enhances scaffold uniformity and reduces average diameter compared to pure PCL scaffolds, which is beneficial for tissue formation, mechanical behavior, and facilitating charge transport critical for electrical conductivity in CTE. FTIR spectra confirm successful PPy incorporation, and mechanical testing demonstrates increased strain capacity, peak stress, and Young's Modulus in PCL+PPy scaffolds. Contact angle measurements indicate water adhesion to PCL+PPy scaffolds, beneficial for cell bioactivity in tissue engineering applications. This research serves as a preliminary step towards the development of a scaffold that could be effectively used in tissue engineering, particularly in CTE, as it combines the biocompatibility of PCL with a conductive polymer in a nanofibrous format.

1. Introduction

The advancements in material science, particularly in the field of polymers, have resulted in ground-breaking developments across various fields. However, in the field of CTE, for example, the use of polymers in electrospun nanofiber scaffolds still reveals certain limitations. Notably, the lack of electrical conductivity restricts intercellular interactions, especially for electroactive cells. Furthermore, their mechanical properties are weaker or significantly different from those of the natural heart. Achieving the optimal level of stiffness to prevent matrix failure during tissue contraction, while maintaining sufficient elasticity to withstand the cyclical stresses of the myocardium, is critical to the success of the scaffold. These parameters play a pivotal role in regulating the behavior of cardiac cells. Achieving successful integration of the scaffold with the host tissue requires correct electrical coupling and ideal mechanical resistance. To address these challenges in CTE, researchers have turned to innovative scaffolds composed of conductive polymers such as poly(3,4 ethylene dioxythiophene) (PEDOT), poly(styrene sulfonate) (PSS), polypyrrole (PPy), and polyaniline (PANI) (Matysiak et al. 2020; Ghovvati et al. 2022; Roshanbinfar et al. 2020), alongside materials like gold nanoparticles and carbon nanotubes or graphene (Bellet et al. 2021; Guo and Ma 2018; Gómez et al. 2021). These developments mark a significant stride in combining material science and biomedical engineering. PPy has gained significant attention due to its remarkable stability, high electrical conductivity, and outstanding intrinsic properties. These characteristics have facilitated diverse applications of PPy, ranging from supercapacitors and biosensors to antistatic coatings and Tissue Engineering (TE). However, the intrinsic mechanical fragility and problematic processability of PPy frequently impede its practical implementation. In recent years, the integration of conductive nanofillers like PPy into engineered cardiac tissues has shown promising improvements. For example, Liang et al.'s study on blending PPy with silk fibroin in electrospun nanofibers resulted in reduced fiber diameter, mechanical properties resembling native myocardium, and sufficient electrical conductivity to support cardiomyocyte contractions (Liang et al. 2021a). Similarly, Zarei et al. achieved conductive scaffolds composed of chitosan, collagen, and polyethylene oxide with PPy as nanofiller, promoting conductivity and facilitating cell

Paper Received: 22 July 2024; Revised: 20 August 2024; Accepted: 21 October 2024
Please cite this article as: Muñoz-Gonzalez A.M., Clavijo-Grimaldo D., 2024, Polypyrrole as a Nanofiller: Comparative Effects on the Properties of Polycaprolactone Scaffolds for Potential Myocardial Tissue Applications, Chemical Engineering Transactions, 114, 1099-1104 DOI:10.3303/CET24114184

adhesion, growth, and proliferation (Zarei et al. 2021). Extending beyond cardiac applications, the versatility of PPy as a nanofiller has been demonstrated in other biomedical fields such as bone and nerve tissue engineering. For instance, Maharjan et al. conducted an in situ polymerization of PPy into a PCL solution, followed by electrospinning the PPy/PCL solution. This process resulted in enhanced mechanical strength, increased surface roughness, decreased fiber diameter, and improved cell behavior, making it suitable for bone tissue application (Maharjan et al. 2020).

Moreover, PPy has been used with polyurethane (PU) and poly-L-lactic acid (PLLA) to obtain a soft conductive, flexible biomaterial that support the proliferation of human skin keratinocytes (Cui, Mao, Rouabhia, et al. 2021). Additionally, PPy combined with PLA has been used in nerve tissue engineering to improve conductivity, hydrophilicity, and mechanical properties of nerve cells (Li, Yu, and Li 2022; Imani et al. 2021).

This study aims to incorporate PPy into nanofibrous polymeric fibers of Polycaprolactone (PCL), a polymer known for its biocompatibility, to assess the impact of PPy particles on the properties of PCL-based scaffolds. Two types of scaffolds were created via electrospinning: a scaffold made of pure PCL nanofibers and a unique combination of PCL and PPy particles (PCL+PPy). Analyzing these samples involved Scanning Electron Microscopy (SEM), Fourier Transform Infrared Spectroscopy (FTIR), tensile strength testing, and contact angle measurements.

2. Materials and Methods

2.1 Materials

PCL (Sigma-Aldrich, CAS # 134490-19-0 MW=80000 Da), isopropyl alcohol (Sigma Aldrich, 99,7 % CAS # 67-66-3), chloroform (Sigma Aldrich, 99,5 %, CAS # 67-66-3) and, PPy (Sigma Aldrich, conductivity 10-50 S/cm, CAS # 30604-81-0).

2.2 Addition of Electro-Conductive Particles

As shown in Figure 1, scaffolds incorporating conductive particles were created by preparing a 9% (w/v) PCL solution in a 50:50 (v/v) chloroform and isopropanol solvent, which was prepared at least 48 hours prior to use (Clavijo-Grimaldo et al. 2022). Subsequently, PPy nanofiller particles were added at a concentration of 1% (w/v) to the prepared PCL solution. To ensure uniform dispersion of the particles within the solution, mixing was conducted using an ultrasonic probe processor designed for low volume applications (Cole-Palmer # EW-04714-53).

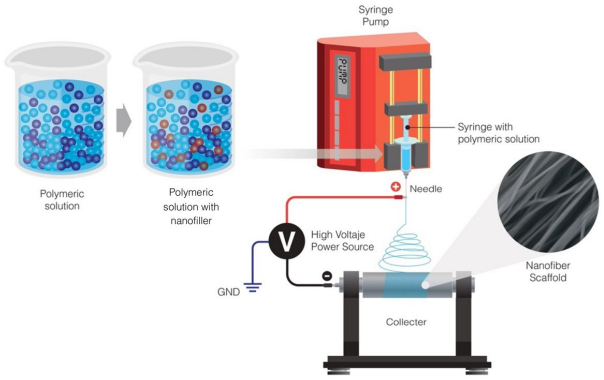

Figure 1 Electroconductive PPy particles incorporation into the electrospun fibers.

To fabricate the scaffold incorporating PCL fibers with PPy particles nanofiller, an electropinning setup was utilized, comprising a high voltage source (CZE1000R, Spellman, USA), a dosing pump (KDS100, USA) with a 5 mL syringe and an 18-gauge needle. The fibers were collected on an aluminum foil rotatory collector at 250 rpm. Key electrospinning parameters optimized included the distance between the needle and the rotary collector, the applied voltage, and the solution feed rate. Ultimately, successful deposition was achieved after 60 minutes at 15 cm distance, 15 kV, and 1.0 ml/h, conducted at a room temperature of 20 °C and 50% relative humidity.

2.3 Characterization of Scaffolds

The morphology and microstructure of the PCL and PCL+PPy scaffolds were examined using a Tescan Vega 3 SB Scanning Electron Microscope (SEM). Images were captured at magnifications of 500X and 5000X using an accelerating voltage of 15 kV to analyze fiber formation and topology. The distribution of fiber diameters was

quantitatively analyzed from the 5000X magnified SEM images using Image J software. Statistical analyses were performed to determine the mean fiber diameter and standard deviation across the sample population.
A Shimadzu® FT-IR spectrometer equipped with an Attenuated Total Reflectance (ATR) module, utilizing a germanium crystal, was employed to assess the chemical functional groups present in the scaffolds. FTIR spectra were acquired in transmission mode over a wavenumber range of 4000 - 500 cm-1 at room temperature. This analysis enabled the identification of polymer-specific bonds and potential interactions between PCL and PPy.The tensile strength of the scaffolds was evaluated using a Shimadzu UH-I Universal Testing Machine with a 50 N load cell. Tests were conducted at a constant rate of 50 mm/min. Rectangular samples measuring 120 mm in length and 10 mm in width were prepared following the ASTM D882 standard procedure. A total of five samples were tested from each scaffold type to ascertain the average mechanical properties, including tensile strength and elongation at break.
Surface hydrophilicity was assessed through water contact angle measurements. A 50 µl drop of deionized water was carefully placed on the surface of each scaffold, and the contact angle was measured using the contact angle plug-in for ImageJ software. The plug-in utilizes sphere and ellipse approximations to calculate the angle formed by a liquid droplet on a solid surface. Three independent points on each sample were measured to provide an average value, and results were expressed as the mean ± standard deviation.

3. Results and discussion

In Figure 2, SEM images showcase the scaffolds alongside their fiber diameter distribution. The PCL scaffold exhibits an average fiber diameter of 1471.52 ± 519.22 nm, with significant size variability. Conversely, the PCL+PPy composite scaffold presents a reduced average diameter of 1056.73 ± 238.99 nm, as substantiated by Figure 2b and d, which depict a more symmetric and centrally clustered diameter distribution, thus more desirable for fostering a homogeneous and predictable tissue formation. This aspect can be crucial for the mechanical function and integration of the tissue.

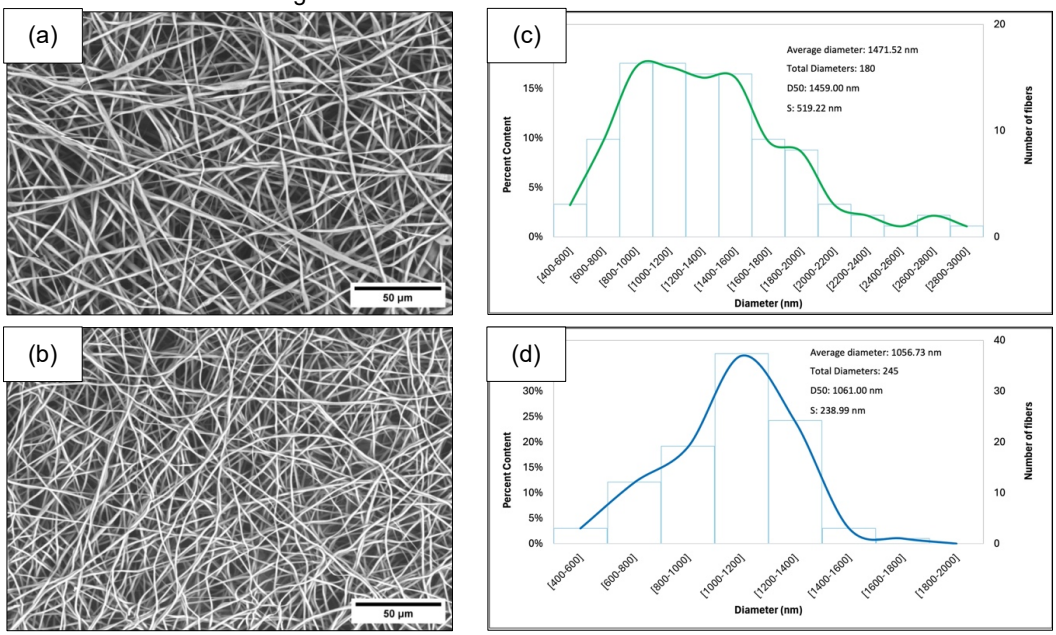

Figure 2 (a) SEM images of the PCL scaffold, (b) fiber diameter distribution of the PCL scaffold, (c) SEM images of the PCL+PPy scaffold, (d) Distribution of the fiber diameter of the PCL+PPy scaffold. D50 is the diameter when the cumulative percentage reaches 50% and S is the standard deviation.

Furthermore, Figure 2a and c, illustrate that fibers containing the PPy nanofiller exhibit greater morphological uniformity compared to those composed solely of PCL. This uniformity could enhance charge transport, resulting in more consistent electrical conductivity throughout the scaffold, which is paramount for the development of more efficacious scaffolds for CTE (Liang et al. 2021b). Here, electrical signaling is crucial for cellular coordination and functionality (Kai et al. 2011). Moreover, this scaffold structure may possess the capacity to support cardiac contractions and convey mechanical forces like natural cardiac tissue. Additionally, the thinner fibers might reduce the scaffold's rigidity due to their lower moment of inertia, thereby offering better resistance to deformation under applied loads (Moroni, de Wijn, and van Blitterswijk 2006).

Furthermore, the SEM images reveal a stochastic yet uniform fiber arrangement, constituting a 3D network in both variants, with the fibers appearing homogeneous and devoid of defects. The incorporation of the PPy modulates the polymeric matrix, reducing its diameter, and consequently enhancing its porosity. This alteration also affects the surface area of the scaffold (Cortez Tornello et al. 2014). It is also discernible that both variants exhibit a porous and interconnected structure, which would likely facilitate vascularization—a key factor in promoting the integration and nourishment of the implanted tissue.

The reduction in diameter is attributed to the inherently electroconductive properties of PPy, which increase the conductivity in the solution, leading to more charge carriers. This amplifies the elongation of the Taylor cone during formation and consequently narrows the fiber diameter (Yan and Gevelber 2010). This diminution is beneficial as it escalates the surface area and porosity of the scaffold—traits that are pivotal in CTE applications because they enhance cell adhesion, nutrient transport, and integration with native tissue (Fioretta et al. 2014). Additionally, even though the diameter of the PCL+PPy scaffold is smaller than that of the PCL scaffold, it effectively emulates the diameter of perimysial fibers, which are about 1 µm. Furthermore, it has been demonstrated that cardiomyocytes cultured on microscale fiber scaffolds exhibit increased propagation and elongation, both at the level of individual cells and within the designed tissue structures (Fleischer et al. 2015).

FTIR assays were used to confirm the presence of the PCL and the PPy particles. In Figure 3 (a) are the FTIR spectra for both PCL and PCL+PPy samples. The PCL spectrum is characterized by prominent peaks: asymmetric CH2 stretching at 2946 cm^{-1}, symmetric CH2 stretching at 2860 cm^{-1}, carbonyl (C=O) stretching at 1717 cm^{-1}, C-C stretching at 1233 cm^{-1}, asymmetric C-O-C stretching at 1166 cm^{-1}, and symmetric COC stretching at 1047 cm^{-1}. These peaks are consistent with previous research (Da Silva et al., 2013; Heidari et al., 2017; Tayebi et al., 2021; Yuan et al., 2012).

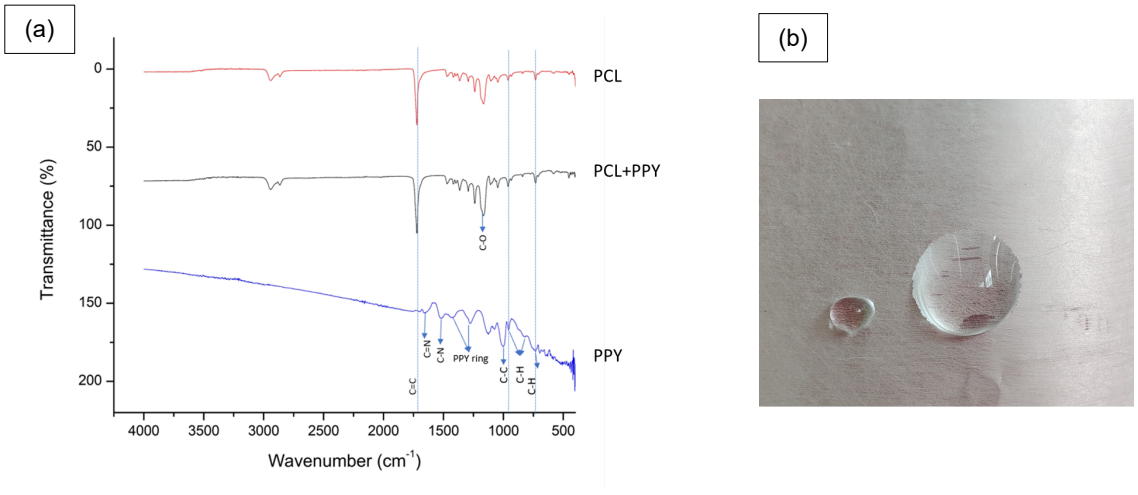

Figure 3 (a) FTIR spectra of PCL, PCL+PPy and PPy.FTIR spectra of PCL, PCL+PPy and PPy. (b) Drop of water on the surface of the PCL+PPy scaffold in vertical position.

In the PPy spectrum, characteristic peaks were discerned at 1678 cm^{-1} indicative of C-N bonds, and at 1548 cm^{-1} denoting to C=C and C-C stretching of the polypyrrole ring. Additional peaks at 1420, 1275 and 1132 cm^{-1} are attributed to C-N bonds within the molecule. Subtle peaks ranging between 954 and 725 cm^{-1} imply C-H bonding in both PCL and PPy molecules, aligning with established literature. (Liang and Goh 2020; Cui, Mao, Zhang, et al. 2021; Yussuf et al. 2018; Shinde et al. 2014). The results demonstrated consistency in the chemical composition of the polymers and confirmed the incorporation of PPy within the scaffolds. Although the FTIR spectrum of the PCL+PPy closely resembles that of pure PCL, this is attributed to the relatively low concentration of PPy. Consequently, minor variations are observed in the PCL+PPy spectrum, indicative of interactions between the two polymers. These interactions are beneficial, as evidenced by the enhancement in both the morphological and mechanical properties of the scaffold.

The wettability of the scaffold surfaces can be determined using the contact angle measurements. For the PCL scaffold the contact angle is 125.38±4.89° and the PCL+PPy scaffold at 127.57±4.65°. The addition of PPy resulted in an increased contact angle, indicating that the surface became more hydrophobic. This change could affect how the scaffold interacts with biological components in TE applications. The hydrophobicity of the scaffold may influence cell adherence, protein absorption, and overall bioactivity. These factors are significant for the scaffold's performance in biomedical applications.Even though the scaffold surfaces are hydrophobic, in the PCL+PPy scaffold water drops tend to attach to the surface, as can be seen in Figure 3 (b). This

phenomenon, in which the water droplet does not flow easily but appears to 'stick' to the surface, may indicate the presence of adhesive forces or surface roughness that increases water retention.
The mechanical properties of the scaffolds were assessed using stress-strain curves, which indicated distinct behaviors between PCL and PCL+PPy, as depicted in Figure 4a. In addition, as demonstrated in Figure 4b, the strain capacity of the PCL+PPy scaffold reached 129.79, in contrast to the PCL scaffold 102.15, suggesting enhanced elasticity. Moreover, the PCL+PPy exhibited a higher peak stress at 3.32 MPa, surpassing the PCL scaffold's 2.50 MPa, indicative of increased resistance. The Young's Modulus of the PCL+PPy scaffold rose to 32.79 MPa from 27.01 MPa for PCL, reflecting a more rigid composite material. It also displayed greater toughness, attributed to the necessity of more energy to fracture a greater volume of material, despite a reduced fiber diameter.These achieved properties also correlate with the microstructure of the scaffolds; the thicker PCL fibers possess greater tensile strength up to the point of failure due to a larger cross-sectional area bearing the load (Moroni, de Wijn, and van Blitterswijk 2006). Conversely, the thinner fibers might facilitate greater deformation before failure, indicating increased ductility of the material. Furthermore, the mechanical properties of the PCL+PPy scaffold are also enhanced due to the improved diameter distribution, resulting in more uniform mechanical characteristics throughout the scaffold.

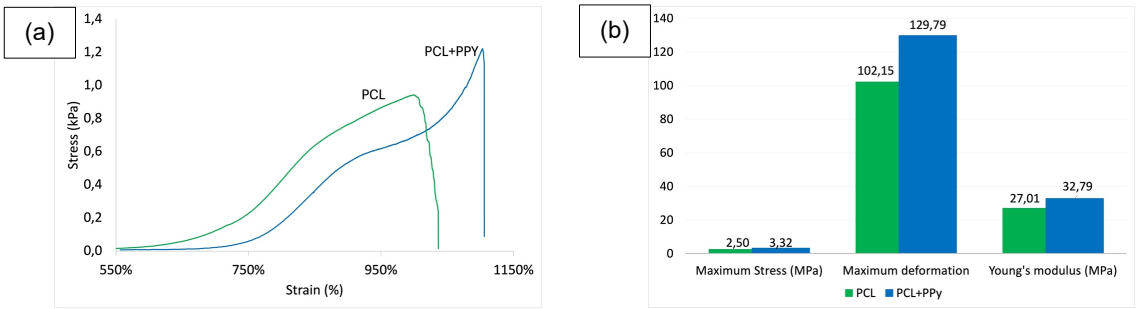

Figure 4 (a) Stress-strain diagram (b) Mechanical properties of the PCL and PCL+PPy scaffolds.

4. Conclusions

This study aimed to explore the integration of PPy, a conductive polymer, into PCL nanofiber scaffolds for potential application in CTE. Through the process of electrospinning, two types of scaffolds were successfully fabricated: one composed of pure PCL nanofibers and another integrating PPy nanoparticles with PCL (PCL+PPy). SEM images confirmed that PCL+PPy scaffolds maintained a fibrous and porous structure, with a reduced average fiber diameter compared to pure PCL scaffolds, enhancing porosity and surface area. This could potentially lead to improved cell adhesion and proliferation. FTIR spectroscopy revealed that PPy was successfully incorporated within the PCL matrix. Although spectral differences were subtle due to the low concentration of PPy, minor peak variations indicated a positive interaction between the two polymers. Tensile testing demonstrated that PCL+PPy scaffolds had superior mechanical properties with increased strain capacity and maximum stress levels. The Young's Modulus was higher for PCL+PPy scaffolds, suggesting a stiffer yet more elastic material suitable for the dynamic cardiac environment. Improving the hydrophilic properties of PCL+PPy scaffolds could further enhance their performance in biological environments, promoting better integration with native tissues and potentially reducing inflammatory responses. This research represents a preliminary yet significant step towards bridging the gap between material science and biomedical applications. The developed PCL+PPy scaffolds exhibit properties that could potentially meet the demands of myocardial tissue, indicating promise for future CTE advancements.

References

Bellet, Pietro, Matteo Gasparotto, Samuel Pressi, Anna Fortunato, Giorgia Scapin, Miriam Mba, Enzo Menna, and Francesco Filippini. 2021. “Graphene-Based Scaffolds for Regenerative Medicine.”

Clavijo-Grimaldo, Dianney, Ciro Alfonso Casadiego-Torrado, Juan Villalobos-Elías, Adolfo Ocampo-Páramo, and Magreth Torres-Parada. 2022. “Characterization of Electrospun Poly(ε-Caprolactone) Nano/Micro Fibrous Membrane as Scaffolds in Tissue Engineering: Effects of the Type of Collector Used.” Membranes 12 (6). https://doi.org/10.3390/membranes12060563.

Cortez Tornello, Pablo R., Pablo C. Caracciolo, Teresita R. Cuadrado, and Gustavo A. Abraham. 2014. “Structural Characterization of Electrospun Micro/Nanofibrous Scaffolds by Liquid Extrusion Porosimetry: A Comparison with Other Techniques.” Materials Science and Engineering C 41 (August):335–42. https://doi.org/10.1016/j.msec.2014.04.065.

Cui, Shujun, Jifu Mao, Mahmoud Rouabhia, Saïd Elkoun, and Ze Zhang. 2021. “A Biocompatible Polypyrrole Membrane for Biomedical Applications.” RSC Advances 11 (28): 16996–6. https://doi.org/10.1039/d1ra01338f.

Fioretta, Emanuela S, Marc Simonet, Anthal I P M Smits, Frank P T Baaijens, and Carlijn V C Bouten. 2014. “Differential Response of Endothelial and Endothelial Colony Forming Cells on Electrospun Scaffolds with Distinct Microfiber Diameters.” Biomacromolecules 15 (3): 821–29. https://doi.org/10.1021/bm4016418.

Fleischer, Sharon, Jacob Miller, Haley Hurowitz, Assaf Shapira, and Tal Dvir. 2015. “Effect of Fiber Diameter on the Assembly of Functional 3D Cardiac Patches.” Nanotechnology 26 (29). https://doi.org/10.1088/0957-4484/26/29/291002.

Ghovvati, M., M. Kharaziha, R. Ardehali, and N. Annabi. 2022. “Recent Advances in Designing Electroconductive Biomaterials for Cardiac Tissue Engineering.” Advanced Healthcare Materials, no. 2200055.

Gómez, Jénnifer, Manuel Vásquez, Daniele Mantione, and Nuria Alegret. 2021. “Carbon Nanomaterials Embedded in Conductive Polymers : A State of the Art.”

Guo, Baolin, and Peter X. Ma. 2018. “Conducting Polymers for Tissue Engineering.” Review-article. Biomacromolecules 19 (6): 1764–82. https://doi.org/10.1021/acs.biomac.8b00276.

Imani, Fatemeh, Reza Karimi-Soflou, Iman Shabani, and Akbar Karkhaneh. 2021. “PLA Electrospun Nanofibers Modified with Polypyrrole-Grafted Gelatin as Bioactive Electroconductive Scaffold.” Polymer 218 (September 2020): 123487. https://doi.org/10.1016/j.polymer.2021.123487.

Kai, Dan, Molamma P. Prabhakaran, Guorui Jin, and Seeram Ramakrishna. 2011. “Polypyrrole-Contained Electrospun Conductive Nanofibrous Membranes for Cardiac Tissue Engineering.” Journal of Biomedical Materials Research - Part A 99 A (3): 376–85. https://doi.org/10.1002/jbm.a.33200.

Li, Siqi, Xiaoling Yu, and Yuan Li. 2022. “Conductive Polypyrrole-Coated Electrospun Chitosan Nanoparticles / Poly (D , L-Lactide) Fibrous Mat : Influence of Drug Delivery and Schwann Cells Proliferation Conductive Polypyrrole-Coated Electrospun Chitosan Nanoparticles / Poly (D , L-Lactide) Fi.” Biomedical Physics & Engineering Express 8.

Liang, Yeshi, and James Cho-Hong Goh. 2020. “Polypyrrole-Incorporated Conducting Constructs for Tissue Engineering Applications: A Review.” Bioelectricity 2 (2): 101–19. https://doi.org/10.1089/bioe.2020.0010.

Liang, Yeshi, Aleksandr Mitriashkin, Ting Ting Lim, and James Cho Hong Goh. 2021a. “Conductive Polypyrrole-Encapsulated Silk Fibroin Fibers for Cardiac Tissue Engineering.” Biomaterials 276 (January): 121008. https://doi.org/10.1016/j.biomaterials.2021.121008.

Maharjan, Bikendra, Vignesh Krishnamoorthi Kaliannagounder, Se Rim Jang, Ganesh Prasad Awasthi, Deval Prasad Bhattarai, Ghizlane Choukrani, Chan Hee Park, and Cheol Sang Kim. 2020. “In-Situ Polymerized Polypyrrole Nanoparticles Immobilized Poly(ε-Caprolactone) Electrospun Conductive Scaffolds for Bone Tissue Engineering.” Materials Science and Engineering C 114 (April): 111056. https://doi.org/10.1016/j.msec.2020.111056.

Matysiak, Wiktor, Tomasz Tański, Weronika Smok, Klaudiusz Gołombek, and Ewa Schab-Balcerzak. 2020. “Effect of Conductive Polymers on the Optical Properties of Electrospun Polyacrylonitryle Nanofibers Filled by Polypyrrole, Polythiophene and Polyaniline.” Applied Surface Science 509 (December 2019). https://doi.org/10.1016/j.apsusc.2019.145068.

Moroni, L, J R de Wijn, and C A van Blitterswijk. 2006. “3D Fiber-Deposited Scaffolds for Tissue Engineering: Influence of Pores Geometry and Architecture on Dynamic Mechanical Properties.” Biomaterials 27 (7): 974–85. https://doi.org/https://doi.org/10.1016/j.biomaterials.2005.07.023.

Roshanbinfar, Kaveh, Lena Vogt, Florian Ruther, Judith A Roether, Aldo R Boccaccini, and Felix B Engel. 2020. “Nanofibrous Composite with Tailorable Electrical and Mechanical Properties for Cardiac Tissue Engineering” 1908612. https://doi.org/10.1002/adfm.201908612.

Shinde, Sujata S., Girish S. Gund, Deepak P. Dubal, Supriya B. Jambure, and Chandrakant D. Lokhande. 2014. “Morphological Modulation of Polypyrrole Thin Films through Oxidizing Agents and Their Concurrent Effect on Supercapacitor Performance.” Electrochimica Acta 119:1–10. https://doi.org/10.1016/j.electacta.2013.10.174.

Yan, Xuri, and Michael Gevelber. 2010. “Investigation of Electrospun Fiber Diameter Distribution and Process Variations.” Journal of Electrostatics 68 (5): 458–64. https://doi.org/https://doi.org/10.1016/j.elstat.2010.06.009.

Yussuf, Abdirahman, Mohammad Al-Saleh, Salah Al-Enezi, and Gils Abraham. 2018. “Synthesis and Characterization of Conductive Polypyrrole: The Influence of the Oxidants and Monomer on the Electrical, Thermal, and Morphological Properties.” International Journal of Polymer Science 2018. https://doi.org/10.1155/2018/4191747.

Zarei, Maryam, Abdolreza Samimi, Mohammad Khorram, Mahnaz M. Abdi, and Seyyed Iman Golestaneh. 2021. “Fabrication and Characterization of Conductive Polypyrrole/Chitosan/Collagen Electrospun Nanofiber Scaffold for Tissue Engineering Application.” International Journal of Biological Macromolecules 168:175–86. https://doi.org/10.1016/j.ijbiomac.2020.12.031.